chapter five

Extracellular electrical stimulation of central neurons: quantitative studies

Dongchul C. Lee, Cameron C. McIntyre, and Warren M. Grill

Contents

5.1 Introduction

Electrical activation of the nervous system is a method to restore function to persons with neurological disorders due to disease or injury and a technique to study the form and function of the nervous system. Application of electrical stimulation, in the form of neural prostheses, is used to restore both motor and sensory functions. Although restoration of motor function has primarily been accomplished by activation of peripheral motor nerve fibers (i.e., last-order neurons), to restore complex motor functions it may be advantageous to access the nervous system at a higher level and use the intact neural circuitry to control the individual elements of the motor system,[22] which may be accomplished by intraspinal microstimulation.[17] Similarly, restoration of the sense of vision may be accomplished by intracortical stimulation in the visual cortex,[3,55] and restoration of the sense of hearing by stimulation of the ventral cochlear nucleus.[30]

In applications of central nervous system (CNS) stimulation, electrodes are positioned in geometrically and electrically complex volume conductors (the brain and spinal cord) containing cell bodies, dendrites, and axons in close proximity. When a stimulus is applied within the CNS, cells and fibers over an unknown volume of tissue are activated, resulting in direct excitation as well as trans-synaptic excitation/inhibition from stimulation of presynaptic axons and cell bodies. Fundamental knowledge of the interactions between the applied currents and the neurons of the CNS has been limited, and this void will impair the development of safe and effective future devices. In this chapter we review the issues that arise during stimulation of the CNS and use quantitative computational modeling to establish a foundation upon which to build future applications of electrical stimulation in the brain. We will focus on two fundamental questions that arise during CNS stimulation:

1. What elements are stimulated by extracellular electrodes in the CNS?
2. What methods will enable selective stimulation of different neuronal elements in the CNS?

5.1.1 What elements are stimulated in the CNS?

The question of what elements are stimulated by extracellular electrodes in the CNS was addressed in the seminal review of Ranck,[45] and we revisit and expand upon the findings set forth in that review. The neuronal elements of interest (Figure 5.1) include local cells around the electrode, including those

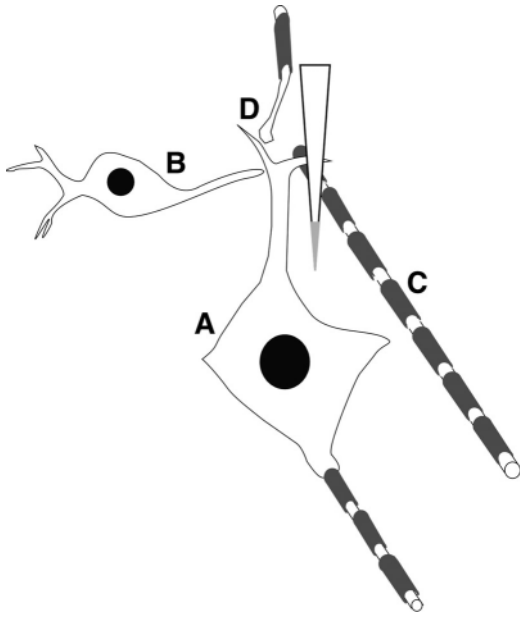

Figure 5.1 During electrical stimulation of the central nervous system, electrodes are positioned within heterogeneous populations of neuronal elements. Neuronal elements that can be activated by stimulation include local cells around the electrode projecting away from the region of stimulation (A), local cells around the electrode projecting locally (B), axons passing by the electrode (C), and presynpatic terminals projecting onto neurons in the region of the electrode (D).

projecting locally around the electrode as well as those projecting away from the region of stimulation, axons passing by the electrode, and presynaptic terminals projecting onto neurons in the region of the electrode. Effects of stimulation can be mediated by activation of any or all of these elements and include direct effects of stimulation of postsynaptic elements, as well as indirect effects mediated by electrical stimulation of presynaptic terminals that mediate the effects of stimulation via synaptic transmission.

Previous experimental evidence demonstrates that different neuronal elements have similar thresholds for extracellular stimulation and illustrates the need for the design of methods that would enable selective stimulation. *In vitro* measurements in cortical brain slices indicate that cells and fibers have similar thresholds for activation.[36,37] Similarly, *in vivo* measurements using microstimulation indicate that fibers and cells have similar thresholds for cathodic rectangular stimuli.[23,45,51] Recent computational studies of the excitation of CNS neurons indicate that, with conventional rectangular stimuli, axons of passage and local cells respond at similar thresholds.[32,33] Also, the thresholds for generating direct and synaptic excitation of neurons in the spinal cord,[23] red nucleus,[4] and cortex[26] were quite similar. Extracellular activation of type-identified spinal motoneurons indi-

cated that the current amplitude necessary to induce repetitive firing with a monopolar electrode was not significantly different for type-S and type-F motoneurons,[58] and modeling results demonstrated a very small difference between the extracellular thresholds of different sized neurons.[33] Thus, with conventional stimulation techniques, the thresholds for activation of different neuronal elements are quite similar, and it is difficult to isolate stimulation of particular neurons.

5.1.2 *Selective stimulation of CNS elements*

A neural prosthesis using microstimulation of the CNS will require selective and controlled activation of specific neural populations. The "complexity of the spinal circuitry implies that if a supraspinal trigger could generate movement it would need to be a highly focused drive onto a select populations of interneurons."[7] Similarly, interpretation of physiological investigations employing microstimulation requires knowledge of the effects of stimulation on different neuronal elements. Application of extracellular currents may activate or inactivate (block) neurons and or axons dependent on their morphology, distance from the electrode, orientation with respect to the electrode, and discharge rate, as well as the stimulus parameters.[45] Effects on cells may differ from the effects on fibers of passage, and fiber activation will result in both antidromic and orthodromic propagation. While the technology for fabrication of high-density arrays of microelectrodes for insertion in the CNS has advanced greatly,[2,9] our knowledge of neuronal activation patterns has not. Advancing our understanding of neuronal excitation and determining what is required to target excitation we will provide useful design parameters for microelectrode arrays.

5.1.3 *Computational modeling as a tool for understanding and design*

Computational modeling provides a powerful tool to study extracellular excitation of CNS neurons. The volume of tissue stimulated, both for fibers and cells, and how this volume changes with electrode geometry, stimulus parameters, and the geometry of the neuronal elements are quite challenging to determine experimentally. Using a computer model enables examination of these parameters under controlled conditions. Neural modeling provides a powerful tool to address the effects of stimulation on all the different neural elements around the electrode simultaneously. Further, well-designed modeling studies enable generation of experimentally testable hypotheses regarding the effects of stimulation conditions on the pattern and selectivity of neuronal stimulation within the CNS. However, the strengths of modeling are tempered by the necessary simplifications made in any reasonable model. In turn, modeling should be coupled as closely as possible to experimental work enabling a synergistic analysis of results.

The utility of such an approach has been demonstrated by previous field-neuron models of cochlear stimulation which were able to replicate experimental activation patterns and document the effects of changes in electrode geometry and stimulus parameters.[14–16] Similarly, integrated field-neuron models of epidural spinal cord stimulation have been used to explain clinical patterns of paresthesias[10,11,57,59] and to design novel electrode geometries for selective stimulation of targeted neural elements.[25,60] These examples demonstrate the utility of computer-based modeling in understanding and controlling neural elements activated by electrical stimulation.

5.2 Quantitative models of CNS neurons

5.2.1 Physical basis of models: from cells to circuits

Neural cells in the CNS are highly varied in their form and function but all share the properties of excitability and polarization. Excitability is based on selective ion channels and polarization is based on the concentration differences of ions, generated by ionic pumps, across the cell membrane. According to Robertson's proposition,[52] all membranes or major portions of membranes have a common basic structure. This structure includes a lipid bilayer covered by non-lipid monolayers on both sides. Within the lipid bilayer reside proteins, and transmembrane proteins form the pores that enable ionic current across the membrane. The electrical properties of the membrane are similar to those of a parallel RC circuit, the so-called *passive membrane*, where the capacitor represents the lipid bilayer and the resistor represents the transmembrane ion channels.

The excitability of neurons comes from the ion channels. Ion channels contribute to changing the conductance across the membrane by passing specific ions. The conductance of some ion channels is dependent on the voltage across the membrane and thus can be considered as nonlinear resistors.[24] The nonlinear properties of ion channels, such as the sodium channel, can produce regenerative coupling to the transmembrane potential by the greatly increased conductance to sodium ions. This nonlinear property in conductance of specific ions is referred to as *active membrane*.

The passive and active properties are the basic components of the membrane throughout the neuron including the cell body, dendrites, and axon. The dendrite and axon are long cylindrical tubes filled with cytoplasm, which has a higher electrical conductivity than the extracellular fluid. Also, for axons and dendrites the electric current flowing through the membrane is much less than the current flowing parallel to the cylinder axis because the resistance of the membrane is much higher than the cytoplasmic resistance. Therefore, the nerve cell with passive membrane properties (i.e., not considering nonlinear ion channels) can be considered a good conductor insulated by a membrane that has high resistivity and a certain capacity. This analog bridges the investigation of electrophysiological properties of neurons to cable theory (Figure 5.2).

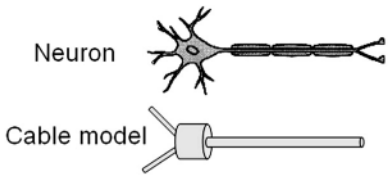

Figure 5.2 Typical neuron and cable model. The passive electrical properties of the dendrites, soma, and axon are similar to the core cable with insulation.

5.2.2 Geometric properties of a range of CNS neurons

The types of neurons in the CNS are exceedingly diverse and are classified into three large groups by shape as unipolar, bipolar, and multipolar neurons. Each group has common features of dendrite and axon structure with respect to the cell body. The morphology of neurons has an impact on their response to extracellular stimulation because the entire neuron is exposed to the electric field. Therefore, the response of the cell is modulated by influences from every branch exposed to the electric field. Table 5.1 shows examples of mammalian CNS neurons to indicate the range of cell structure and size.

5.2.3 Cable models of CNS neurons

Cable theory was first presented in 1855 by William Thomson, who provided the mathematical derivation and applications for submarine telegraphic cables. This theory included both steady-state and transient solutions for particular boundary conditions and initial conditions.[27,41] The solution was for a single spatial dimension that facilitated the theoretical treatment of transient as well as steady-state solutions. The theory was applied for nerve electronus by Matteucci in 1863 and further developed by Hermann in the 1870s.

5.2.4 Cable equation: continuous form

The continuous form of the cable equation is derived from a compartment model that consists of a series of compartments, each with a resistance and a capacitance.[41] Each compartment represents a segment of cable with the length of Δx, and all properties such as resistance and capacitance in the segment are lumped into one element for each (Figure 5.3). The cable equation is derived by application of Kirchoff's current law (KCL) — conservation of currents — which states that the difference in the currents (between i_{i1} and i_{i2}) in the axial direction is the current flowing through the membrane (Figure 5.4). Mathematically this is expressed as:

$$i_{i1} - i_{i2} = -\Delta i_i = i_m \Delta x$$

The membrane current ($i_m \Delta x$) is the sum of two components: the resistive current $V_m(\Delta x / r_m)$ and the capacitive current $c_m \Delta x((\partial V_m)/(\partial t))$. Therefore, the membrane current is given by:

Table 5.1 Range of Geometrical Properties of CNS Neurons

Region	Neuron	Ref.	Mean Soma Diameter (μm)	Number of Dendrite Stems on Soma	Dendritic Terminal Length (μm)
Cerebellum	Purkinje cell	Roth and Hauser[54]	50 ~ 80	2 ~ 10	50 ~ 200
Thalamus	TCP neurons	Ohara and Havton[38]	11 ~ 20	4 ~ 8	28 ~ 3000
Hippocampus	Pyramidal cell	Bannister and Larkman;[5] Bilkey and Schwartzkroin[6]	15 ~ 30	2 ~ 8	300 ~ 1000
Retina	Ganglion cell	Sheasby and Fohlmeister[56]	20 ~ 30	3 ~ 7	50 ~ 1000
Spinal cord	Motor neuron	Rose et al.[53]	50 ± 10	10 ± 2	1,150 ± 304

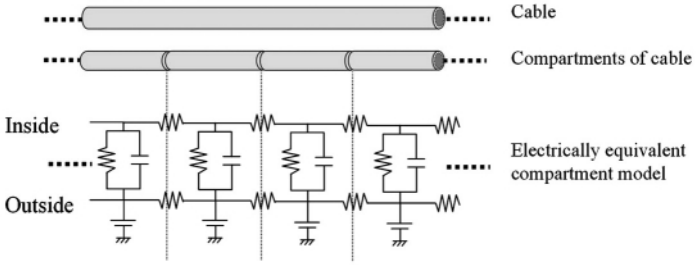

Figure 5.3 Compartment model of cable. Insulation (membrane) around core is equivalent to resistance in parallel with capacitance.

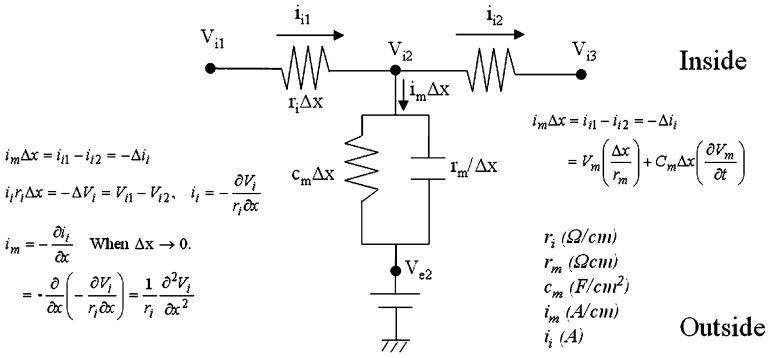

Figure 5.4 Application of Kirchoff's current law at a compartment of a cable model to derive the cable equation. The membrane current includes capacitive and resistive currents, and their sum is equal to the change in the axial current.

$$i_m \Delta x = V_m\left(\frac{\Delta x}{r_m}\right) + c_m \Delta x\left(\frac{\partial V_m}{\partial t}\right)$$

The equation is simplified by dividing Δx on both sides and the result is:

$$i_m = \frac{V_m}{r_m} + c_m\left(\frac{\partial V_m}{\partial t}\right)$$

The axial current, derived from Ohm's law as that current flowing between two consecutive nodes (V_{i1} and V_{i2} or V_{i2} and V_{i3}), is defined by potential difference divided by resistance and expressed as:

$$V_{i1} - V_{i2} = -\Delta V_i = i_i r_i \Delta x$$

$$i_i r_i = -\frac{\Delta V_i}{\Delta x}$$

By taking the limit $\Delta x \to 0$, the axial current is expressed by partial derivative:

$$i_i = -\frac{1}{r_i}\frac{\partial V_i}{\partial x}$$

Going back to KCL, defining conservation of the current, the membrane current with partial derivative form yields:

$$\begin{aligned} i_m &= -\frac{\Delta i_i}{\Delta x} \\ &= -\frac{\partial i_i}{\partial x}, \quad \text{when } \Delta x \to 0 \end{aligned}$$

Therefore, the membrane current is the partial derivative of the axial current with respect to x. Again, the axial current is also a partial derivative of the axial potential distribution by spatial variable x. Applying the axial current equation in partial derivative form $(-(\partial i_i/\partial x))$,the membrane current can be expressed as:

$$i_m = -\frac{\partial i_i}{\partial x} = -\frac{\partial}{\partial x}\left(-\frac{\partial V_i}{r_i \partial x}\right) = \frac{\partial^2 V_i}{r_i \partial x^2}$$

The transmembrane potential (V_m) is defined as $V_i - V_e$, so the intracellular potential V_i can be replaced by $V_m + V_e$. Finally, the current i_m is expressed as:

$$i_m = \frac{\partial^2 V_m}{r_i \partial x^2} + \frac{\partial^2 V_e}{r_i \partial x^2}$$

Combining with the earlier equation for transmembrane current as the sum of the resistive and capacitive current yields:

$$\frac{1}{r_i}\frac{\partial^2 V_m}{\partial x^2} + \frac{1}{r_i}\frac{\partial^2 V_e}{\partial x^2} = \frac{V_m}{r_m} + c_m\left(\frac{\partial V_m}{\partial t}\right)$$

$$\frac{1}{r_i}\frac{\partial^2 V_m}{\partial x^2} - \frac{V_m}{r_m} - c_m\left(\frac{\partial V_m}{\partial t}\right) = -\frac{1}{r_i}\frac{\partial^2 V_e}{\partial x^2}$$

The general single-dimension cable equation is a partial differential equation expressed as:

$$\lambda^2 \frac{\partial^2 V}{\partial x^2} - V - \tau\frac{\partial V}{\partial t} = F$$

where V is the transmembrane voltage as a function of x (spatial variable) and t (time), and $\lambda = \sqrt{r_m / r_i}$ and $\tau = r_m c_m$ are the space and time constants defined by the electrical properties of the neuron. The F represents a forcing function or input caused by synaptic conductance change, applied electric fields, and/or active membrane properties. This nonhomogeneous partial differential equation can be transformed to a homogeneous equation ($F = 0$) with additional initial conditions by the principle of superposition. Further simplification can be made for steady-state conditions by $(\partial V/\partial t) = 0$, which will yield a homogeneous linear second-order ordinary differential equation as $\lambda^2(\partial^2 V/\partial x^2) - V = 0$, the solution of which is a sum of two exponentials (cable of infinite length) or hyperbolic functions (cable of finite length). The solution for a finite cable is:

$$V = B_1 \cosh(\frac{x}{\lambda}) + B_2 \sinh(\frac{x}{\lambda})$$

where B_1 and B_2 are defined by boundary condition at $x = 0$ and $x = l$ (cable length). The equivalent solution for the infinite cable is:

$$V = A_1 \exp(\frac{x}{\lambda}) + A_2 \exp(-\frac{x}{\lambda})$$

where A_1 and A_2 are determined by conditions at $x = 0$ and $x = \pm\infty$. Transient solutions of the cable equation can be obtained by using separation of variables. For a finite-length cable with the boundary condition of sealed ends,[40,43,50] the solution can be expressed as an infinite series:

$$V = \sum_{n=0}^{\infty} B_n \cos(n\pi \frac{x}{\lambda}) \exp(-\frac{t}{\tau} - (\frac{n\pi\lambda}{l})^2 \frac{t}{\tau})$$

$$B_0 = (\frac{1}{l}) \int_0^l V(x, t = 0) dx$$

$$Bn = (\frac{2}{l}) \int_0^l V(x, t = 0) \cos(\frac{n\pi x}{l}) dx,\ n > 0$$

where l and τ are the length of cable and time constant of cable, respectively.

5.2.5 *Cable equation: discrete form*

The continuous form of the cable equation is limited to homogeneous structures with restrictive assumptions. The passive properties of the dendritic tree and unmyelinated axons with constant diameter can be modeled using

the continuous cable equation. However, a typical dendritic tree has various diameters from stem to dendritic terminal, and myelinated axons have different membrane properties at the nodes of Ranvier and in the internodal segments. The nonhomogenous cable properties can be modeled using a discrete form of the cable equation that is a mathematical representation of the compartmental circuit model of a neuron.

The general discrete cable equation is directly derived from the continuous case. The partial derivative of the spatial variable is replaced by Δ, yielding:

$$\frac{1}{r_i}\frac{\Delta^2 V_m}{\Delta x^2} - \frac{V_m}{r_m} - c_m\left(\frac{dV_m}{dt}\right) = -\frac{1}{r_i}\frac{\Delta^2 V_e}{\Delta x^2}$$

This equation is only useful for compartmental models of homogeneous cables, but small modifications of the equation give rise to great flexibility for practical applications such as nonhomogeneous dendrites, cell bodies, and myelinated axons. In the discrete compartmental cable model, the resistance (axial and membrane) and capacitance are not required to be functions of Δx. Therefore, each variable — $1/(r_i\Delta x)$, $c_m\Delta x$, and $\Delta x/r_m$ — can be replaced by $G_a(k\Delta x)$ ($\Omega\angle^1$), $C_m(k\Delta x)$ (F), and $R_m(k\Delta x)$ (Ω). This yields the discrete cable equation applicable to a cable with any geometry. The steady-state solution of the discrete cable equation can be obtained from linear algebra; however, the transient solution must be obtained numerically.

As an example of application of the discrete cable equation, a myelinated axon is considered where the myelin has a very high resistivity (assumed to be an insulator), thus simplifying the model to include only the nodes of Ranvier and the axial resistance (Figure 5.5). Under this circumstance, the cable equation in differential form will be discrete in space and continuous in time. The membrane (nodal) current is defined similarly to the continuous case with a resistive current (G_mV_m) and a capacitive current ($C_m(dV_m/dt)$). The total current flowing through the node of Ranvier is expressed as:

$$I_{node} = G_mV_m + C_m\left(\frac{dV_m}{dt}\right)$$

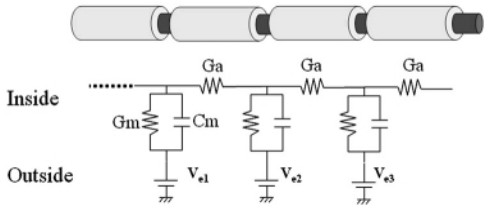

Figure 5.5 Compartmental model of a myelinated axon. The internodal segment is modeled by an axial resistor, because of the highly resistive myelin sheath. The node of Ranvier is lumped into a single compartment, which is a relatively small portion compared to the internodal segment (1.5 μm in length vs. 1 mm in length).

The axial current between successive nodes of Ranvier depends on the internodal conductance (G_a) and potential difference ($V_{i1} - V_{i2}$ or $V_{i2} - V_{i3}$) according to Ohm's law. Just as the membrane current was obtained from the difference of axial currents in the continuous case, the nodal current equation in the discrete model is:

$$\begin{aligned} I_{node} &= I_i - I_2 = Ga \cdot (V_{i1} - V_{i2}) - Ga \cdot (V_{i2} - V_{i3}) \\ &= Ga \cdot (V_{i1} - 2V_{i2} + V_{i3}) \\ &= Ga \cdot (V_{m1} - 2V_{m2} + V_{m3}) + Ga \cdot (V_{e1} - 2V_{e2} + V_{e3}) \end{aligned}$$

where $V_m = V_i - V_e$. Combining this equation with the equation for the components of the membrane current yields:

$$G_m V_m + C_m \left(\frac{dV_m}{dt} \right) = Ga \cdot (V_{m1} - 2V_{m2} + V_{m3}) + Ga \cdot (V_{e1} - 2V_{e2} + V_{e3})$$

Rearranging terms and defining the second difference of the potential as:

$$Ga \cdot (V_{m1} - 2V_{m2} + V_{m3}) = Ga \cdot \Delta^2 V_m$$

yields the discrete cable equation for myelinated axon:

$$G_m V_m + C_m \left(\frac{dV_m}{dt} \right) - Ga \cdot (\Delta^2 V_m) = Ga \cdot \Delta^2 V_e$$

The final equation is similar to the general form of the cable equation with a forcing term of $G_a \cdot \Delta^2 V_e$. For a step change in the extracellular potential from steady state, as would occur by application of a rectangular current pulse, the forcing term will determine initial polarization pattern of the axon, because the $C_m(dV_m/dt)$ term will follow the sign of the forcing term.

5.2.6 *Assumptions*

The cable model and cable equation are good approximations to understand the properties of neurons, but they must be used with the following assumptions:

1. Any angular or radial dependence of V within the core or outside the membrane is neglected. This assumption is reasonable for steady-state solutions of small-diameter cables with high-conductivity cores corresponding to high cytoplasm conductivities. Low conductivity of the cable core will generate a voltage gradient within the cable in

the radial direction and violate this assumption. Practically, the high conductivity of the cytoplasm eliminates this effect. This assumption is also invalid under extracellular stimulation with large diameter cables such as used to represent the soma. The extracellular potentials are dependent on the angular position on the soma,[28,29] and the angular dependence of V is a function of the electrode to cell distance and of the electrode type. Therefore, it is valid only for relatively small diameter cables such as dendrites and axons or cables far from the stimulation electrode.

2. The core conductivity is uniform everywhere (homogeneous medium). This assumption implies that the ratio between the resistivity of cytoplasm and the cross sectional area is constant. For homogeneous cytoplasm, it implies constant diameter of the cable. Practically, the diameters of dendrites and axons may change along their paths. Thus, the morphology of neurons limits direct application of analytical solution of the continuous cable equation and requires discretization to account for geometric inhomogeneity.

5.2.7 *Passive electrical properties of CNS neurons*

In the nervous system, information is transported long distances by action potentials. The action potential is generated by depolarization of the membrane where active ion channels are present. The depolarization can be generated by any input, including synaptic current or current generated by an extracellular electric field. When the degree of polarization from a certain input (voltage or current) is under threshold the neuron will not fire an action potential and can be considered using the so-called *passive electrical properties*. The passive electrical properties are described by the input impedance, the time constant, and the resting potential. The input impedance of the neuron is defined by the relationship between the current applied by an intracellular electrode and the transmembrane voltage response. The input impedance determines how much the transmembrane voltage of neuron will change in response to a steady current:

$$\Delta V = I \times R_{in}$$

As the passive membrane is modeled as a resistance in parallel with a capacitance, the response of the membrane (voltage) takes time to reach steady state. The change in transmembrane potential of the passive membrane can be described by following equation:

$$\Delta V(t) = I_{injected} R_{in} (1 - e^{-t/\tau})$$

where τ is the membrane time constant given by the product of input resistance and input capacitance. The resting potential is determined by the ionic

Table 5.2 Range of Passive Electrical Properties of CNS Neurons

Region	Neuron	Ref.	Input Resistance (MΩ)	Time Constant (msec)	Resting Potential (mV)
Cerebellum	Purkinje cell	Raman and Bean;[44] Roth and Hausser[54]	59.3 ± 38.4	64.6 ± 17.2	–62 ± 3 with 300 n*M* TTX
Thalamus	Thalamocortical neuron	Turner et al.[61]	30 ~ 240	5 ~ 35	–60 ~ –73
Hippocampus	Pyramidal cell	Bilkey and Schwartzkroin[6]	23 ± 2	12.5 ± 0.97	–55.7 ± 1.28
Retina	Ganglion cell	Sheasby and Fohlmeister[56]	800 ~ 1600	47 ~ 85	–64 ~ –66
Spinal cord	Motor neuron	McDonagh et al.[31]	2.5 ~ 32	2.5 ~ 52	–60 ~ –83

concentration difference across the membrane and the states of the ion channels at rest. The balance of ion fluxes gives rise to the resting potential, which is quantified by the Goldman equation. It usually ranges from –60 to –70 mV. The resting potential is a reference point for measurements of changes in transmembrane potential. The range of passive electrical properties of example neurons presented in Table 5.2.

5.2.8 *Intracellular vs. extracellular stimulation*

Properties of neuronal excitation have been studied primarily by intracellular electrical stimulation by injecting current through a glass pipette electrode. The injected current will flow in the axoplasm and pass through membrane, and the neuron can again be modeled using a discrete compartmental cable model (Figure 5.6). The transmembrane voltage at each compartment is determined by current flowing through the membrane and axoplasm, and an analytical solution provides the profile of transmembrane voltage along the cable for different boundary conditions (Figure 5.7).

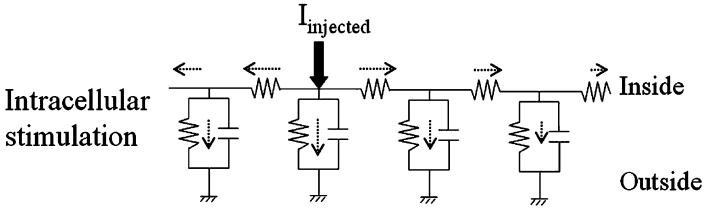

Figure 5.6 Electrically equivalent model to intracellular stimulation. Intracellular stimulation of the nerve cell or fiber is modeled as a cable with a current or voltage source connected to specific locations of the cable. The stimulation corresponds to the forcing term (F) in the cable equation.

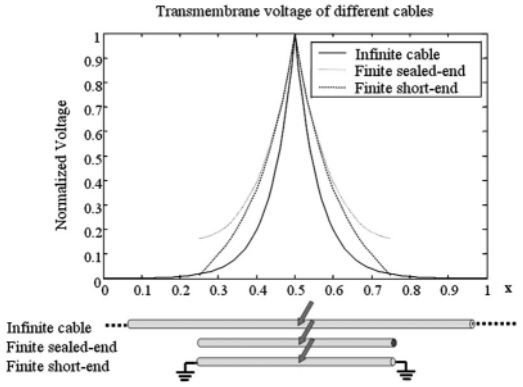

Figure 5.7 Analytical solution of the cable equation with three different boundary conditions to determine the profile of transmembrane potential generated by intracellular current injection.

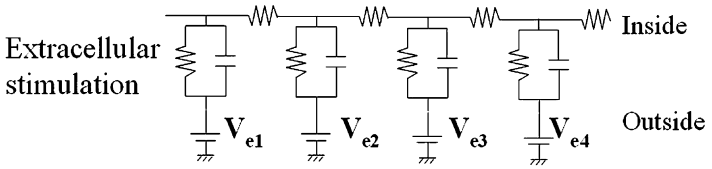

Figure 5.8 Electrically equivalent cable model under extracellular stimulation. The extracellular electrode will determine the extracellular potentials (V_e) along the cable which act as the sources to generate axial and transmembrane currents.

Application of current in the extracellular space (extracellular stimulation) creates a specific pattern of electric field and thus electric potentials along the cable (Figure 5.8). The extracellular potentials (V_e) along the cable are determined by the geometry of the cable, the source geometry and location, and the electrical properties of the extracellular space. As derived in the cable equation,[1,41,48] the second derivative of the extracellular potentials along the cable ($-(1/r_i)\ (\partial^2 V_e/\partial x^2)$) will produce current across the membrane and intracellular axial current and thus changes in transmembrane potential.

Mathematically this forcing term (*activating function*: $(1/r_i)\ (\partial^2 V_e/\partial x^2)$ is equivalent to current injection in each compartment in an equivalent model with intracellular current injections.[48,62] As we derived the continuous and discrete cable equations using Kirchoff's current law, the conservation of current at each node must be satisfied. Under the condition that the second derivative of V_e equals zero, the cable equation is homogeneous and consists of three terms:

$$\frac{1}{r_i}\frac{\partial^2 V_m}{\partial x^2} - \frac{V_m}{r_m} - C_m\left(\frac{\partial V_m}{\partial t}\right) = 0$$

The first term represents the axial current difference, the second represents the membrane resistive current, and the third represents the membrane capacitive current with unit of A/cm.[2] Therefore, the additional term, $-(1/r_i)\ (\partial^2 V_e/\partial x^2)$ arising from the extracellular potentials corresponds to a current (A/cm^2) source connected to each node, as shown in Figure 5.9. If a series of equivalent currents are injected along the cable, the effect of extracellular stimulation is equivalent to the effect of intracellular stimulation with a series of distributed intracellular current sources. The equivalent current at each node can be of anodic or cathodic polarity from a single extracellular electrode, because the forcing term ($G_a \cdot \Delta^2 V_e$) is determined by axon geometry and electrode type and location.[62]

The potentials generated by an extracellular electrode produce both inward and outward transmembrane current in the cable, as shown in Figure 5.10. The direction of transmembrane current depends on the location along the cable and creates regions of both depolarization and hyperpolarization

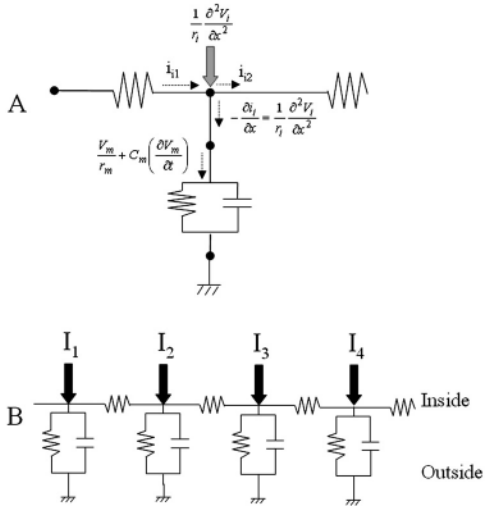

Figure 5.9 Equivalent model of extracellular stimulation with current injection in each compartment. (A) The equivalent current for each compartment is derived from the cable equation with the non-zero V_e using Kirchoff's current law. (B) The extracellular stimulation can be converted to an equivalent model with distributed intracellular current sources.

along the cable, in contrast to the unidirectional polarization resulting from intracellular stimulation (Figure 5.7).

5.2.9 *Source driving polarization*

Solution of the infinite cable equation provides the steady-state voltage distribution along the cable expressed as an exponential function. The change in voltage along the cable is determined by the space constant, which is a function of the ratio between the membrane and cytoplasmic resistivities (Figure 5.7). For realistic dendrites (finite cable with nonhomogeneous geo-

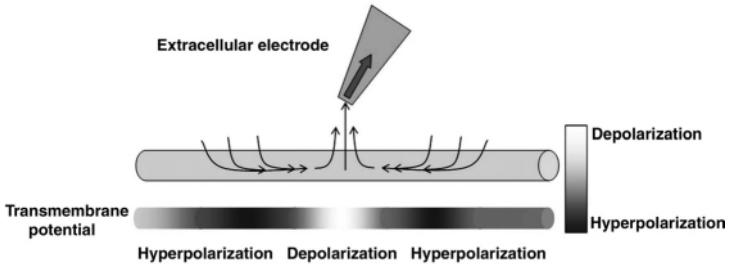

Figure 5.10 Current flow induced by an extracellular current source and polarization pattern (changes in transmembrane potential) along the cable. A cathodic extracellular point-source electrode will depolarize the cable (light) near the electrode and hyperpolarize both sides of the depolarized region (dark).

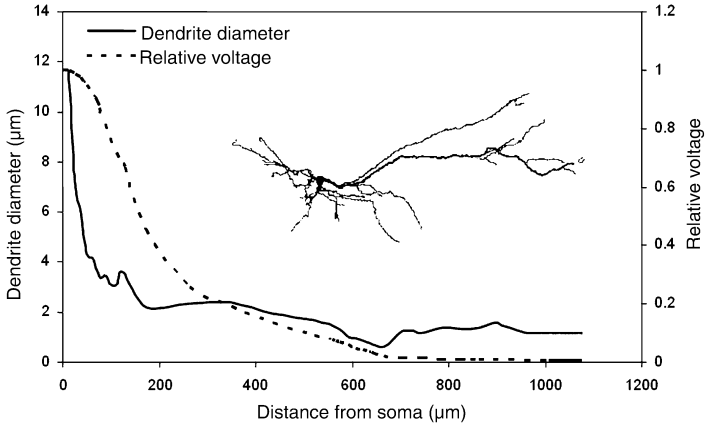

Figure 5.11 Simulation result from the real geometry of dendrite. The voltage profile along the real dendrite is determined by geometric information. This limits the application of theoretical cable equation to realistic dendrites or axon where nonlinear ion channels are located and activated by this voltage change.

metric structure), the voltage distribution depends on the cable geometry. Figure 5.11 illustrates the voltage profile along a long dendritic tree (dark line from cell body to the dendritic terminal) of a preganglionic parasympathetic neuron with a realistic morphology reconstructed from cat spinal cord by Morgan and Ohara.[35] The dendrite diameter changes along the tree and the transmembrane voltage depends on the cable diameter.

Under extracellular stimulation, the transmembrane voltage response depends on the orientation and geometry of the neuron, because the extracellular potential outside each compartment is determined by the type of source and the distance from it. As seen from the cable equation, the source driving polarization is the second derivative of the extracellular potential along the cable and must be non-zero to create changes in membrane potential in the neuron.

As an example the extracellular potential and transmembrane potentials of three myelinated axons under a point current (I) source were calculated using the discrete cable equation (Figure 5.12). The extracellular potential is inversely proportional to the electrode-to-cable distance (R) and is given by:

$$V_e = \frac{I}{4\pi\sigma_e R}$$

where σ_e is the conductivity of the extracellular space with unit of S/cm. The transmembrane potential generated by the point source is triphasic, which is approximately predicted by activating function (see Section 5.2.8). Anodic extracellular stimulation produces maximum hyperpolarization on the nearest point of the cable and two depolarization peaks next to it, while

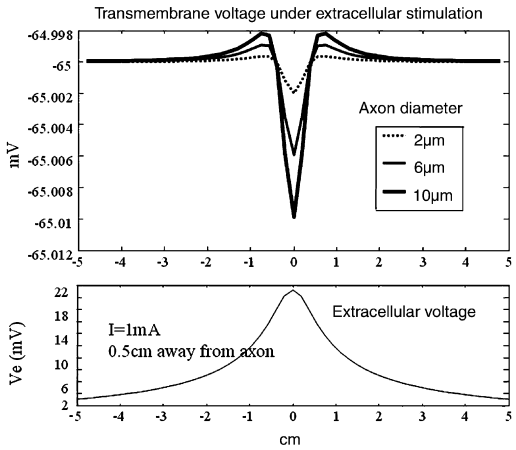

Figure 5.12 Transmembrane voltage of axons induced by extracellular current source and extracellular voltage along the axon. (A) The magnitude of transmembrane voltages (top traces) is proportional to axon diameter, because the larger diameter axon has a larger internodal distance, which will increase activating function by raising the second derivative $\Delta^2 V_e$ and conductance term G_a. (B) Extracellular voltage along the cable is inverse proportional to the electrode to cable distance.

cathodic extracellular stimulation produces the opposite pattern of polarization. Action potential initiation occurs at the point of maximum depolarization and will thus differ under anodic and cathodic stimulation.

5.2.10 *Modeling of synaptic inputs*

Excitation of neurons can be initiated by an extracellular electric field as described, but the behavior of the nerve cell is also modulated by synaptic inputs from presynaptic terminals that are exposed to the extracellular electric field. Because of the large number of connections, input from presynaptic terminals excited by extracellular stimulation can have strong postsynaptic effects (see Section 5.3.2).

Most rapid signaling between nerve cells in the CNS involves ionotropic transmission that occurs through synaptic connections. When an action potential arrives at a presynaptic terminal, depolarization results in release of neurotransmitters into the synaptic cleft. The released neurotransmitters diffuse to the postsynaptic cell membrane where they bind to the receptors. Receptors are activated by specific neurotransmitters and generate excitatory postsynaptic potential (EPSP) or inhibitory postsynaptic potential (IPSP).

As with other ion channels, activation of postsynaptic receptors changes channel conductance, which generates a postsynaptic current described by:

$$I_{syn} = f_{syn}\bar{g}_{syn}(V_{post} - E_{syn})$$

where f_{syn} is fractional transmitter release, $\bar{g}_{syn}$ is maximal postsynaptic conductance, and E_{syn} is the reversal potential.[8,13] A simple form of f_{syn} is modeled using an alpha function:[42]

$$f_{syn}(t) = \frac{t}{t_p}\exp(1-\frac{t}{t_p})$$

This function has rapid rise to a peak at t_p and slow decay with time constant t_p and is a good empirical estimate of the postsynaptic conductance change. As synaptic inputs are modeled as current sources with nonlinear conductances, distribution of synaptic inputs on a modeled postsynaptic neuron corresponds to adding a forcing term in each compartment. These "indirect" synaptic forcing terms may alter the patterns of neural activation due to the "direct" forcing terms arising from extracellular stimulation and cannot be overlooked during CNS stimulation.

5.3 *Properties of CNS stimulation*

To make accurate inferences about anatomical structures or physiological mechanisms involved in electrical stimulation, one must know which neural elements the stimulus pulse activates. When stimulating within the CNS the electrode is placed within a complex volume conductor where there are three general classes of neurons that can be affected: local cells, axon terminals, and fibers of passage (Figure 5.1). Local cells represent neurons that have their cell body in close proximity to the electrode. Axon terminals represent neurons that project to regions near the electrode and make synaptic connections with local cells. Fibers of passage represent neurons where both the cell body and axon terminals are far from the electrode, but the axonal process of the neuron traces a path that comes in close proximity to the electrode. Each of these classes of neurons can be activated by stimulation with extracellular sources. However, activation of each different class can result in different physiologic and/or behavioral outputs. Experimental measurements indicate that local cells, axon terminals, and fibers of passage have similar thresholds for activation when stimulating with extracellular sources (see Section 5.1.1). Therefore, it is often difficult to determine the clear effects of extracellular stimulation.

5.3.1 *Direct activation*

The seminal review of Ranck[45] laid the groundwork for understanding the effects of electrical stimulation within the CNS; however, because of limitations in experimental techniques and the complex response of neurons to extracellular stimulation, our understanding of electrical stimulation of the CNS has advanced at a relatively slow pace. The use of multicompartment cable models of CNS neurons coupled to extracellular electric fields has given us the opportunity to address many important issues related to extracellular

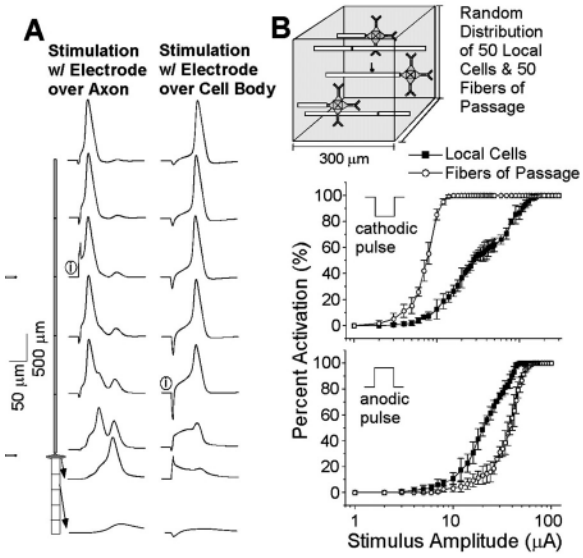

Figure 5.13 Direct excitation of neurons with extracellular stimulation. (A) Action potential initiation (API) and propagation for two different electrode locations (electrode-to-neuron distance of 100 µm) and cathodic stimulus pulses with durations of 0.1 msec. The left and right columns correspond to the responses from electrodes located over the axon or cell body, respectively. Each row shows the transmembrane voltage as a function of time at the segment of the neuron shown to the left. The site of API is noted by the circled *i*. (Modified from McIntyre and Grill.[32]) (B) Input–output relations for populations of neurons stimulated by a monopolar electrode. Excitation was studied using randomly distributed populations of 50 local cells and 50 fibers of passage. Percentages of activated neurons (mean ± one standard deviation from three different random distributions) are displayed as a function of stimulus amplitude for a monophasic cathodic stimulus (pulse duration [pd] = 0.20 msec) and a monophasic anodic stimulus (pd = 0.20 msec). (Modified from McIntyre and Grill.[33])

stimulation, including the site of action potential initiation and the effects of changes in stimulus parameters on activation patterns.[18,19,32–34,46,47] The analysis of modeling and experimental findings results in four general conclusions regarding the effects of stimulation within the CNS (Figure 5.13):

1. When stimulating local cells with extracellular sources, action potential initiation (API) takes place in a node of Ranvier of the axon relatively far away from the electrode (Figure 5.13A).
2. When stimulating axon terminals and fibers of passage with extracellular sources, API takes place in a node of Ranvier relatively close to the electrode (Figure 5.13A).
3. Anodic stimuli are more effective in activating local cells than cathodic stimuli (Figure 5.13B).
4. Cathodic stimuli are more effective in activating fibers of passage and axon terminals than anodic stimuli (Figure 5.13B).

It should always be noted, however, that activation of any neuron with extracellular electric fields is dependent on four main factors:

1. Electrode geometry and the electrical conductivity of the tissue medium — The response of the neuron to stimulation is dependent on the electric field generated by the electrode, which is dependent on the size and shape of the electrode. In addition, the inhomogeneous and anisotropic electrical properties of the CNS tissue medium affect the shape of electric field.[21] Therefore, both the type of electrode used and the region of the CNS where it is inserted will affect the neural response to stimulation.
2. Stimulation parameters — Changes in stimulation parameters can affect the types of neurons activated by the stimulus and the volume of tissue over which activation will occur. The four primary stimulation parameters are the polarity, duration, and amplitude of the stimulus pulse and the stimulus frequency. In general, alterations in the stimulus pulse duration and amplitude will affect the volume of tissue activated by the stimulus, and alterations in the stimulus polarity and frequency will affect the types of neurons activated by the stimulus.
3. Geometry of the neuron and its position with respect to the electrode — In general, the closer the neuron is to the electrode the lower the stimulation current necessary for activation. However, complex neural geometries such as dendritic trees and branching axons result in a large degree of variability in current–distance relationships (threshold current as a function of electrode-to-neuron distance) of the same types of neurons. Therefore, the orientation of the neural structures with respect to the electrode is of similar importance to the geometric distance between them, especially for small electrode-to-neuron distances.
4. Ion channel distribution on the neuron — Axonal elements of a neuron consist of a relatively high density of action-potential-producing sodium channels compared to cell bodies and dendrites. As a result, the axonal elements of a neuron are the most excitable and regulate the neural output that results from application of extracellular electric fields. However, while the cell body and dendrites may not be directly responsible for action potential spiking that results from the stimulus, they do contain several types of calcium and potassium channels that can affect neuronal excitability on long time scales when trains of stimuli are used.

5.3.2 Indirect effects

Previous experimental and modeling results have shown that the threshold for indirect, or trans-synaptically evoked, excitation or inhibition of local cells stimulated with extracellular sources is similar to (in some cases, depen-

dent on electrode location less than) the threshold for direct excitation of local cells (see Section 5.1.1). Indirect excitation or inhibition of local cells is the result of stimulation-induced release of neurotransmitters that results from the activation of axon terminals activated by the stimulus. Axon terminals are activated at low stimulus amplitudes relative to local cells, especially when cathodic stimuli are used. Therefore, when considering the effect of the stimulus on local cells near the electrode it is probable that a large number of axon terminals are activated, resulting in high levels of synaptic activity on the dendritic trees of local cells.

Stimulation-induced trans-synaptic activity can be predominantly excitatory, predominantly inhibitory, or any relative mix of excitation and inhibition, depending on the types and numbers of synaptic receptors activated. Therefore, the interpretation of the effects the stimulation on the neuronal output of local cells is made up of two components: (1) the direct effect of the extracellular electric field on the local cell, and (2) the indirect effect of the stimulation-induced trans-synaptic excitation and/or inhibition. As a result, an action potential can be generated either by the stimulus pulse itself or by indirect synaptic activation. However, activation of axon terminals by extracellular stimuli is nonselective to excitatory or inhibitory neurotransmitter release.

In general, the indirect effects of extracellular stimulation of local cells result in a biphasic response of a short period of depolarization followed by a longer period of hyperpolarization. This biphasic response is the result of the interplay between the time courses of the traditionally fast excitatory synaptic action and the traditionally slow inhibitory synaptic action. The role of indirect effects on the output of local cells can be enhanced with high-frequency stimulation (Figure 5.14). If the interstimulus interval is shorter than the time course of the synaptic conductance, the indirect effects will summate. Because inhibitory synaptic action traditionally has a longer time course than excitatory synaptic action, the effect of this summation is hyperpolarization of the cell body and dendritic arbor of the local cell when high-frequency stimulus trains are used. This hyperpolarization can limit the neuronal output that results from direct effects from the stimulus and can functionally block the ability of the neuron to integrate non-stimulation-induced synaptic activity during the interstimulus interval. However, because action potential initiation takes place in the axon of local cells in response to the direct effects of the stimulation, local cells will still fire action potentials in response to each stimulus pulse given that the stimulus amplitude is strong enough (Figure 5.14C).

5.4 Selective stimulation

Microstimulation in the CNS can activate neurons with greater specificity than is possible with larger electrodes on the surface of the spinal cord or brain. The potential thus arises for electrical activation of intact neuronal circuitry, and, in turn, generation of distributed and controlled physiological outputs

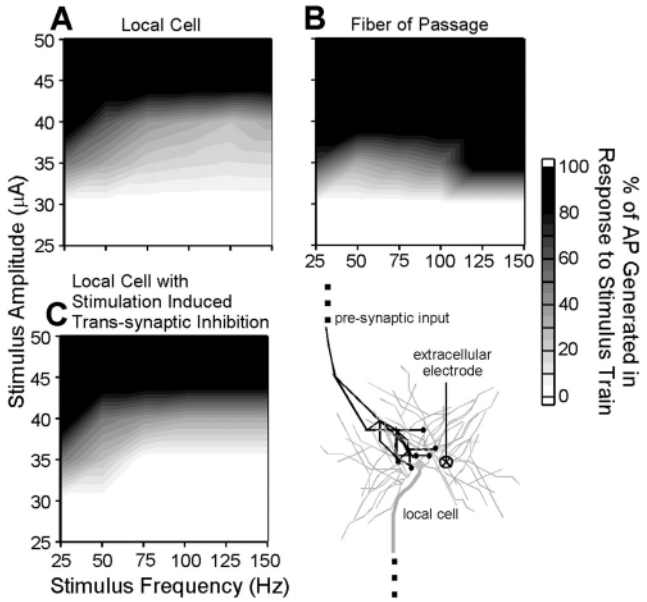

Figure 5.14 Neuronal output as a function of stimulus amplitude and frequency. Neuronal output (percentage of stimuli in a 500-msec stimulus train that generate propagating action potentials in the neuron models) was quantified for direct excitation of a local cell (A) and a fiber of passage (B) from a train of charge-balanced, cathodic-phase first symmetrical biphasic stimuli (100 μsec per phase). Both neurons had a threshold for activation from a single pulse of 34 μA. (C) Influence of stimulation-induced trans-synaptic inhibition on the neuronal output of the local cell. Each terminal of the presynaptic input was activated by a stimulus, and in turn synaptic conductances representative of GABAergic inhibition were applied to the dendrites of the local cell following each stimulus in the train. (Modified from McIntyre and Grill.[34])

for the study of the neural control of function or for application in neural prostheses. However, in many regions of the CNS, local cells, axon terminals, and fibers of passage are intermingled in close proximity to the electrode. In general, only one class of neurons is the target population to achieve the desired output from the stimulus. Yet, the stimulation used to activate the target neurons (e.g., local cells) can also result in activation of the other classes of neurons around the electrode (e.g., axon terminals, fibers of passage). Therefore, techniques that can enable selective activation of target populations of neurons with little to no activation of non-target populations can improve our understanding of experimental results using electrical stimulation of the CNS and provide important tools for application in neuroprosthetic devices.

Previous modeling and experimental work have shown that local cells have lower thresholds for activation with anodic stimuli, while axonal elements (axon terminals and/or fibers of passage) have lower thresholds with cathodic stimuli (Figure 5.13B);[32,33,45] however, chronic application of electrical stimulation within the nervous system requires the use of biphasic stimuli because of

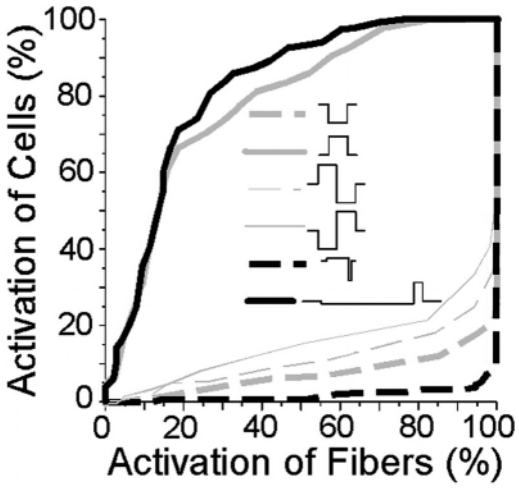

Figure 5.15 Selective activation of targeted neuronal populations via alterations in the stimulus waveform. Using randomly distributed populations of neurons (Figure 5.1B), we examined the effect of changes in the stimulus waveform on the relative activation of local cells compared to fibers of passage. Plotted is the percentage activation of local cells as a function of the percentage activation of fibers of passage for six different stimulus waveforms. The stimulus waveforms (from top to bottom in Figure 5.5; see caption) consisted of a monophasic cathodic pulse (pulse duration [pd] = 0.2 msec), a monophasic anodic pulse (pd = 0.2 msec), a symmetrical anode first biphasic pulse (pd = 0.2 msec for each phase), a symmetrical cathode first biphasic pulse (pd = 0.2 msec for each phase), an asymmetrical anode first biphasic pulse (pd = 0.2 msec for anodic phase; 0.02 msec for cathodic phase), and an asymmetrical cathode first biphasic pulse (pd = 1 msec for cathodic phase; 0.1 msec for anodic phase). (Modified from McIntyre and Grill.[33])

issues related to tissue damage and electrode corrosion.[39] In general, when biphasic stimuli are used, local cells or axonal elements will be activated during the anodic or cathodic phases of the stimulus, respectively, resulting in low selectivity for activation of a target population (Figure 5.15).[33] Alterations in the stimulus frequency and/or stimulus waveform represent techniques that can enable enhanced selectivity of either local cells or axonal elements.

5.4.1 *Effect of stimulus frequency*

Mammalian neurons exhibit both depolarizing and hyperpolarizing afterpotentials that follow an action potential spike. The time course of these afterpotentials is different in the cell body and axon, and these afterpotentials affect the threshold for generation of subsequent impulses.[34] Myelinated axons exhibit a relatively long-duration (~15 msec), high-amplitude (~5 mV) depolarizing afterpotential (DAP) followed by a long-duration (~80 msec), low-amplitude (~1 mV) afterhyperpolarization (AHP). Neuronal cell bodies traditionally exhibit a shorter duration, lower amplitude

DAP that is followed by a pronounced AHP on the order of ~5 to 10 mV that reaches its maximum ~10 to 20 msec after the action potential spike. During the DAP of the myelinated axon, the threshold to generate another action potential is decreased, and during the AHP of the neuronal cell body the threshold to generate another action potential is increased. The overlap in time course of these afterpotentials for the exploitation of biophysical differences in local cells and fibers of passage to enhance selectivity.

Figure 5.14 shows the responses of a neuron with its cell body near the electrode compared to the response of a fiber of passage to symmetrical biphasic stimulus trains.[34] Maps of the percent of stimuli that generated propagating action potentials during the stimulus train as a function of stimulus amplitude and frequency were generated. Both the local cell (Figure 5.14A) and fiber of passage (Figure 5.14B) can fire in response to the first stimulus in the train when the stimulus amplitude is greater than or equal to 34 μA. However, the near-threshold stimulus amplitudes, the ability of either the local cell or the fiber of passage to follow the stimulus train in a one-to-one ratio is affected by the different time courses and amplitudes of the afterpotentials in the two neurons.

These results demonstrate that modulation of the frequency of the stimulus train can enhance selectivity between activation of cells and fibers of passage within the CNS. However, it should be noted that while the selectivity of fibers of passage can be increased with high-frequency stimulation, local cells can still respond to the stimulus, albeit at a lower average rate. The limited output of the local cells from high-frequency stimulation could still be great enough to generate a functional activation of their efferent target, and, conversely, driving fibers of passage over 100 Hz may exceed the physiological limits for those neurons and result in unexpected or unwanted affects. In addition, the output of local cells at high stimulus frequencies is dependent not only on its direct excitation characteristics but also on the role of indirect trans-synaptic influences (Figure 5.14C). Therefore, while modulation of stimulation frequency can enhance selectivity of fibers of passage over cells, this technique is not especially effective without the augmentation of alterations in the stimulus waveform.

5.4.2 *Effect of stimulus waveform*

The stimulating influence of extracellular electric fields is related to the second difference of the extracellular potential distribution on the surface of the individual neurons, and this stimulating influence will cause regions of both depolarization and hyperpolarization in the same cell.[32,46,47] In general, when stimulating local cells API occurs in the axon of the neuron, relatively far from the electrode, while when stimulating axonal elements (axon terminals and/or fibers of passage) API occurs in a region of the fiber relatively close to the electrode (Figure 5.13A). Stimulus waveforms can be used that exploit the nonlinear conductance properties of the neural elements of local cells and axonal elements. Due to geometrical and biophysical factors, API

in local cells takes place in neural elements that are hyperpolarized by cathodic stimuli and depolarized by anodic stimuli.[32] As a result, monophasic anodic stimuli are more effective in activating local cells than monophasic cathodic stimuli (Figure 5.13B); however, fibers of passage are stimulated more effectively with cathodic stimuli than anodic stimuli (Figure 5.13B). Yet, chronic stimulation requires the use of biphasic stimulus waveforms.[39] Therefore, asymmetrical charge-balanced biphasic stimulus waveforms have been developed to selectively activate either local cells or axonal elements.[33]

Stimulus waveforms capable of selectively activating either local cells or axonal elements use a long-duration, low-amplitude, pre-pulse phase followed by a short-duration, high-amplitude, stimulation phase. The long-duration, pre-pulse phase of the stimulus is designed to create a subthreshold depolarizing pre-pulse in the neural element, where excitation will take place in the non-target neurons, and a hyperpolarizing pre-pulse in the neural element, where excitation will take place in the target neurons.[33] The effect of this subthreshold polarization is to decrease the excitability of the non-target population and increase the excitability of the target population via alterations in the degree of sodium channel inactivation.[20] Therefore, when the stimulation phase of the waveform is applied (opposite polarity of the pre-pulse), the target neuronal population will be activated with enhanced selectively compared with monophasic stimuli (Figure 5.15). Further, charge balancing is achieved as required to reduce the probability of tissue damage and electrode corrosion.

Figure 5.15 shows the effects of changing the stimulus waveform on the activation of populations of local cells and fibers of passage randomly distributed around the stimulating electrode.[33] As seen in Figure 5.13B, monophasic anodic or cathodic stimuli result in selective activation of local cells or fibers of passage, respectively. However, when symmetrical charge-balanced biphasic stimuli are used, selectivity is diminished. Asymmetrical, charge-balanced, biphasic, cathodic-phase first stimulus waveforms result in selective activation of local cells, and asymmetrical, charge-balanced, biphasic, anodic-phase first stimulus waveforms result in selective activation of fibers of passage. However, even with the appropriate stimulus waveform it should always be noted that selective activation of either local cells or axonal elements is affected by the stimulation-induced, trans-synaptic influences on the local cells.

5.5 *Conclusion*

Electrical stimulation of the CNS is a powerful tool to study neuronal connectivity and physiology, as well as a promising technique to restore function to persons with neurological disorders. However, the complexity of central volume conductors (brain and spinal cord) and the neuronal elements (cells, axons, dendrites) therein has limited our understanding of CNS stimulation. To understand the results of studies employing CNS stimulation requires knowledge of which neuronal elements are affected

by stimulation, and optimizing neural prosthetic interventions requires techniques that enable selective stimulation of targeted neuronal populations. Computational modeling is a powerful tool to address both the question of what neuronal elements are activated by CNS stimulation and to design optimal interventions.

Acknowledgments

Preparation of this chapter was supported by NIH Grant R01-NS-40894.

References

1. Altman, K.W. and Plonsey, R., Development of a model for point source electrical fibre bundle stimulation, *Med. Biol. Eng. Comput.*, 26, 466–475, 1988.
2. Anderson, D.J., Najafi, K., Tanghe, S.T., Evans, D.A., Levy, K.L., Hetke, J.F., Xue, X., Zappia, J.J., and Wise, K.D., Batch fabricated thin-film electrodes for stimulation of the central auditory system, *IEEE Trans. Biomed. Eng.*, 36, 693–698, 1989.
3. Bak, M., Girvin, J.P., Hambrecht, F.T., Kufta, C.V., Loeb, G.E., and Schmidt, E.M., Visual sensations produced by intracortical microstimulation of the human occipital cortex, *Med. Biol. Eng. Comput.*, 28(3), 257–259, 1990.
4. Baldissera, F., Lundberg, A., and Udo, M., Stimulation of pre- and postsynaptic elements in the red nucleus, *Exp. Brain Res.*, 15, 151–167, 1972.
5. Bannister, N.J. and Larkman, A.U., Dendritic morphology of CA1 pyramidal neurones from the rat hippocampus. II. Spine distributions, *J. Comp. Neurol.*, 360, 161–171, 1995.
6. Bilkey, D.K. and Schwartzkroin, P.A., Variation in electrophysiology and morphology of hippocampal CA3 pyramidal cells, *Brain Res.*, 514, 77–83, 1990.
7. Burke, D., Movement programs in the spinal cord [commentary], *Behav. Brain Sci.*, 15, 722, 1992.
8. Calabrese, R., Hill, A., and VanHooser, S., Realistic modeling of small neuronal circuits, in *Computational Neuroscience*, DeSchutter, E., Ed., CRC Press, Boca Raton, FL, 2001, pp. 259–288.
9. Campbell, P.K., Jones, K.E., Huber, R.J., Horch, K.W., and Norman, R.A., A silicone-based three-dimensional neural interface: manufacturing processes for an intracortical electrode array, *IEEE Trans. Biomed. Eng.*, 38, 758–767, 1991.
10. Coburn, B., Electrical stimulation of the spinal cord, two-dimensional finite element analysis with particular reference to epidural electrodes, *Med. Biol. Eng. Comput.*, 18, 573–584, 1980.
11. Coburn, B., A theoretical study of epidural electrical stimulation of the spinal cord. II. Effects on long myelinated fibers, *IEEE Trans. Biomed. Eng.*, 32, 978–986, 1985.
12. Coburn, B. and Sin, W.K., A theoretical study of epidural electrical stimulation of the spinal cord. I. Finite element analysis of stimulus fields, *IEEE Trans. Biomed. Eng.*, 32, 971–977, 1985.
13. Destexhe, A., Mainen, Z., and Sejnowski, T., An efficient method for computing synaptic conductances based on a kinetic model of receptor binding, *Neural Comput.*, 6, 14–18, 1994.

14. Finley, C.C., Wilson, B.S., and White, M.W. Models of neural responsiveness to electrical stimulation, in *Cochlear Implants: Models of the Electrically Stimulated Ear*, Miller, J.M. and Spelman, F.A., Eds., Springer-Verlag, New York, 1990, pp. 55–96.
15. Frijns, J.H.M., de Snoo, S.L., ten Kate, J.H., Spatial selectivity in a rotationally symmetric model of the electrically stimulated cochlea, *Hearing Res.*, 95, 33–48, 1996.
16. Frijns, J.H.M., de Snoo, S.L., and Schoonhoven, R., Potential distributions and neural excitation patterns in a rotationally symmetric model of the electrically stimulated cochlea, *Hearing Res.*, 87, 170–186, 1995.
17. Giszter, S.F., Grill, W.M., Lemay, M.A., Mushahwar, V., and Prochazka, A., Intraspinal microstimulation, techniques, perspectives and prospects for FES, in *Neural Prostheses for Restoration of Sensory and Motor Function*, Moxon, K.A. and Chapin, J.K., Eds., CRC Press, Boca Raton, FL, 2001, pp. 101–138.
18. Greenberg, R.J., Velte, T.J., Humayun, M.S., Scarlatis, G.N., and de Juan E., A computational model of electrical stimulation of the retinal ganglion cell, *IEEE Trans. Biomed. Eng.*, 46, 505–514, 1999.
19. Grill, W.M. and McIntyre, C.C., Extracellular excitation of central neurons, implications for the mechanisms of deep brain stimulation, *Thalamus Related Syst.*, 1, 269–277, 2001.
20. Grill, W.M. and Mortimer, J.T., Stimulus waveforms for selective neural stimulation, *IEEE Eng. Med. Biol.*, 14, 375–385, 1995.
21. Grill, W.M., Modeling the effects of electric fields on nerve fibers influence of tissue electrical properties, *IEEE Trans. Biomed. Eng.*, 46, 918–928, 1999.
22. Grill, W.M., Electrical activation of spinal neural circuits, application to motor-system neural prostheses, *Neuromodulation*, 3, 89–98, 2000.
23. Gustafsson, B. and Jankowska, E., Direct and indirect activation of nerve cells by electrical pulses applied extracellularly, *J. Physiol.*, 258, 33–61, 1976.
24. Hodgkin, A.L. and Katz, B., The effect of sodium ions on the electrical activity of the giant axon of the squid, *J. Physiol. (London)*, 108, 37–77, 1949.
25. Holsheimer, J., Nuttin, B., King, G.W., Wesselink, W.A., Gybels, J.M., and de Sutter, P., Clinical evaluation of paresthesia steering with a new system for spinal cord stimulation, *Neurosurgery*, 42, 541–547, 1998.
26. Jankowska, E., Padel, Y., and Tanaka, R., The mode of activation of pyramidal tract cells by intracortical stimuli, *J. Physiol.*, 249, 617–636, 1975.
27. Kelvin, W.T., On the theory of the electric telegraph, *Proc. Roy. Soc. London*, 7, 382–399, 1855.
28. Lee, D. and Grill, W., Polarization of a spherical cell in a non-uniform electric field: transient response and comparison with polarization in a uniform field, in press.
29. Lee, D. and Grill, W., Polarization of a spherical cell in a nonuniform electric field: steady state analysis, *Ann. Biomed. Eng.*, 29(suppl.), S-128, 2001.
30. McCreery, D.B., Shannon, R.V., Moore, J.K., and Chatterjee, M., Accessing the tonotopic organization of the ventral cochlear nucleus by intranuclear microstimulation, *IEEE Trans. Rehabil. Eng.*, 6, 391–9, 1998.
31. McDonagh, J.C., Gorman, R.B., Gilliam, E.E., Hornby, T.G., Reinking, R.M., and Stuart, D.G., Electrophysiological and morphological properties of neurons in the ventral horn of the turtle spinal cord, *J. Physiol. Paris*, 93, 3–16, 1999.
32. McIntyre, C.C. and Grill, W.M., Excitation of central nervous system neurons by nonuniform electric fields, *Biophys. J.*, 76, 878–888, 1999.

33. McIntyre, C.C. and Grill, W.M., Selective microstimulation of central nervous system neurons, *Ann. Biomed. Eng.*, 28, 219–233, 2000.
34. McIntyre, C.C. and Grill, W.M., Extracellular stimulation of central neurons: influence of stimulus waveform and frequency on neuronal output, *J. Neurophysiol.,* 88, 1592–1604, 2002.
35. Morgan, C.W. and Ohara, P.T., Quantitative analysis of the dendrites of sacral preganglionic neurons in the cat, *J. Comp. Neurol*., 437, 56–69, 2001.
36. Nowak, L.G. and Bullier, J., Axons, but not cell bodies, are activated by electrical stimulation in cortical gray matter. I. Evidence from chronaxie measurements, *Exp. Brain Res.,* 118, 477–488, 1998.
37. Nowak, L.G. and Bullier, J., Axons, but not cell bodies, are activated by electrical stimulation in cortical gray matter. II. Evidence from selective inactivation of cell bodies and axon initial segments, *Exp. Brain Res.,* 118, 489–500, 1998.
38. Ohara, P.T. and Havton, L.A., Dendritic architecture of rat somatosensory thalamocortical projection neurons, *J. Comp. Neurol*., 341, 159–171, 1994.
39. Pudenz, R.H., Bullara, L.A., Jacques, S., and Hambrecht, F.T., Electrical stimulation of the brain. III. The neural damage model, *Surg. Neurol.,* 4, 389–400, 1975.
40. Rall, W. and Rinzel, J., Branch input resistance and steady attenuation for input to one branch of a dendritic neuron model, *Biophys. J.*, 13, 648–687, 1973.
41. Rall, W., Cable theory for neurons, in *Handbook of Physiology,* Kandel, E.R., Ed., American Physiological Society, Bethesda, MD, 1977, pp. 39–97.
42. Rall, W., Distinguishing theoretical synaptic potentials computed for different soma-dendritic distributions of synaptic input, *J. Neurophysiol*., 30, 1138–1168, 1967.
43. Rall, W., Time constants and electrotonic length of membrane cylinders and neurons, *Biophys. J.*, 9, 1483–1508, 1969.
44. Raman, I.M. and Bean, B.P., Ionic currents underlying spontaneous action potentials in isolated cerebellar Purkinje neurons, *J. Neurosci*., 19, 1663–1674, 1999.
45. Ranck, J.B., Which elements are excited in electrical stimulation of mammalian central nervous system: a review, *Brain Res.,* 98, 417–440, 1975.
46. Rattay, F., Analysis of the electrical excitation of CNS neurons, *IEEE Trans. Biomed. Eng.*, 45, 766–772, 1998.
47. Rattay, F., The basic mechanism for the electrical stimulation of the nervous system, *Neuroscience*, 89, 335–346, 1999.
48. Rattay, F., Analysis of models for extracellular fiber stimulation, *IEEE Trans. Biomed. Eng*., 36, 676–682, 1989.
50. Rinzel, J. and Rall, W., Transient response in a dendritic neuron model for current injected at one branch, *Biophys. J.*, 14, 759–790, 1974.
51. Roberts, W.J. and Smith, D.O., Analysis of threshold currents during microstimulation of fibers in the spinal cord, *Acta Physiol. Scand*., 89, 384–394, 1973.
52. Robertson, J.D., Unit membranes, in *Cellular Membranes in Development*, Locke, M., Ed., Academic Press, New York, 1964.
53. Rose, P.K., Keirstead, S.A., and Vanner, S.J., A quantitative analysis of the geometry of cat motoneurons innervating neck and shoulder muscles, *J. Comp. Neurol*., 239, 89–107, 1985.

54. Roth, A. and Hausser, M., Compartmental models of rat cerebellar Purkinje cells based on simultaneous somatic and dendritic patch-clamp recordings, *J. Physiol.*, 535, 445–472, 2001.
55. Schmidt, E.M., Bak, M.J., Hambrecht, F.T., Kufta, C.V., O'Rourke, D.K., and Vallabhanath, P., Feasibility of a visual prosthesis for the blind based on intracortical microstimulation of the visual cortex, *Brain*, 119(pt. 2), 507–522, 1996.
56. Sheasby, B.W. and Fohlmeister, J.F., Impulse encoding across the dendritic morphologies of retinal ganglion cells, *J. Neurophysiol.*, 81, 1685–1698, 1999.
57. Sin, W.K. and Coburn, B., Electrical stimulation of the spinal cord: a further analysis relating to anatomical factors and tissue properties, *Med. Biol. Eng. Comput.*, 21, 264–269, 1983.
58. Spielmann, J.M., Laouris, Y., Nordstrom, M.A., Robinson, G.A., Reinking, R.M., and Stuart, D.G., Adaptation of cat motoneurons to sustained and intermittent extracellular activation, *J. Physiol.*, 464, 75–120, 1993.
59. Struijk, J.J., Holsheimer, J., van Veen, B.K., and Boom, H.B.K., Epidural spinal cord stimulation: calculation of field potentials with special reference to dorsal column nerve fibers, *IEEE Trans. Biomed. Eng.*, 38, 104–110, 1991.
60. Struijk, J.J., Holsheimer, J., Spincemaille, G.H.G.H., Gielen, F.L., and Hoekema, R., Theoretical performance and clinical evaluation of transverse tripolar spinal cord stimulation, *IEEE Trans. Rehab. Eng.*, 6, 277–285, 1998.
61. Turner, J.P., Anderson, C.M., Williams, S.R., and Crunelli, V., Morphology and membrane properties of neurones in the cat ventrobasal thalamus *in vitro*, *J. Physiol.*, 505(pt. 3), 707–726, 1997.
62. Warman, E.N., Grill, W.M., and Durand, D., Modeling the effects of electric fields on nerve fibers: determination of excitation thresholds, *IEEE Trans. Biomed. Eng.*, 39, 1244–1254, 1992.